

Environmental Research Letters



LETTER

Non-uniform changes in different categories of precipitation intensity across China and the associated large-scale circulations

OPEN ACCESS

RECEIVED

11 August 2018

REVISED

14 November 2018

ACCEPTED FOR PUBLICATION

22 November 2018

PUBLISHED

1 February 2019

Original content from this work may be used under the terms of the [Creative Commons Attribution 3.0 licence](#).

Any further distribution of this work must maintain attribution to the author(s) and the title of the work, journal citation and DOI.

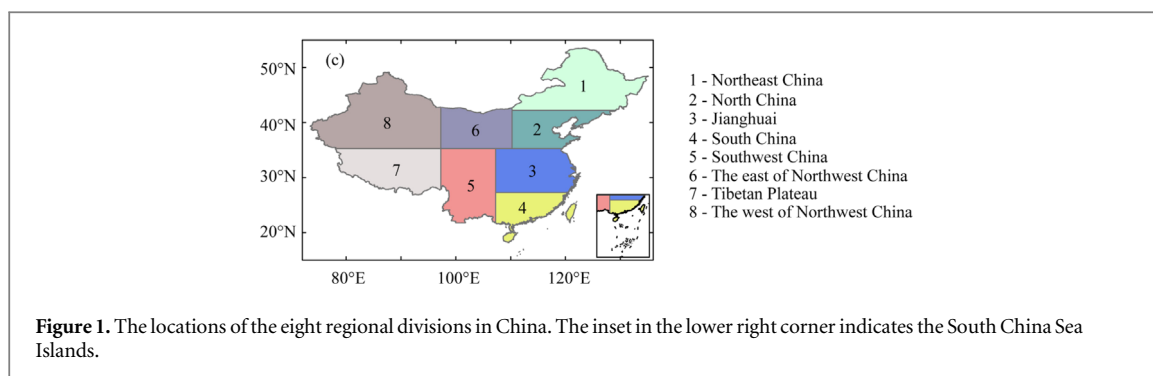
Chiyan Miao¹ , Qingyun Duan¹, Qiaohong Sun¹, Xiaohui Lei² and Hu Li³¹ State Key Laboratory of Earth Surface Processes and Resource Ecology, Faculty of Geographical Science, Beijing Normal University, Beijing 100875, People's Republic of China² State Key Laboratory of Simulation and Regulation of Water Cycle in River Basin, China Institute of Water Resources and Hydropower Research, Beijing 100038, People's Republic of China³ Key Laboratory of Agricultural Non-point Source Pollution Control, Ministry of Agriculture/Institute of Agricultural Resources and Regional Planning, Chinese Academy of Agricultural Sciences, Beijing 100081, People's Republic of ChinaE-mail: miaocy@vip.sina.com**Keywords:** non-uniform changes, precipitation, China, large-scale circulation**Abstract**

This study focuses on changing trends in precipitation across mainland China during the period 1957–2014. We explore the influence of the El Niño–Southern Oscillation (ENSO), the Pacific Decadal Oscillation (PDO), and related large-scale atmospheric circulation variables on the changes in precipitation. The number of wet days showed statistically significant downward trends in North China, Jianghuai, South China, and Southwest of China, but upward trends on the Tibetan Plateau and in Northwest China. However, the number of very wet days increased in Jianghuai, South China and regions in Southwest China, and there was an increase in the spatial variability of a number of rainfall extremes over China. Because the changes in the frequency of wet days and very wet days were non-uniform, an increasing percentage of the total annual precipitation was derived from extreme events over large regions of mainland China. The ENSO and the PDO had a zonal influence on precipitation variability through the modulation of large-scale atmospheric circulation. Both the number of wet days and the frequency of extreme precipitation increased in southern Jianghuai and South China in El Niño years compared with La Niña years. A decrease (increase) in the number of wet days was observed in northern China (southeastern China) during positive PDO-phase years, which was likely a response to the large decrease in Southerly winds.

1. Introduction

Under global warming, the hydrological cycle is likely to intensify, resulting in changes in the characteristics of precipitation. A number of studies have investigated the spatiotemporal changes in precipitation (Ma *et al* 2015, Sun *et al* 2018). Recently, studies have suggested a complex and spatially heterogeneous pattern of precipitation changes (Ghosh *et al* 2011, Donat *et al* 2013, Rajah *et al* 2014). Due to the complex terrain, the climate over China varies greatly in both space and time (Xu *et al* 2015, Miao *et al* 2016b). Previous studies revealed that the frequency of light and moderate precipitation events decreased across China as a whole over the period 1960–2013, whereas there were upward trends in the frequency of very heavy events

(Ma *et al* 2015). Southeastern and northeastern China experienced a wetting tendency owing to an increase in precipitation intensity, whereas southwestern China showed a significant drying tendency (Xiao *et al* 2017). Over southwest China, the changes in precipitation extremes displayed spatial heterogeneity with the decreasing spatial variability of precipitation extremes during the 1959–2012 period (Liu *et al* 2015). Pre-existing research mainly looked into trends in mean precipitation and precipitation extremes, or on overall changes in different categories of precipitation. Few studies have quantitatively assessed the spatial variability of different categories of precipitation across China. Such studies, together with investigations into the underlying mechanisms, are essential and



meaningful for disaster and water management (Ghosh *et al* 2011, Liu *et al* 2015, Miao *et al* 2016a).

The variability of precipitation over China is believed to be related to a number of factors, including the El Niño–Southern Oscillation (ENSO) and the Pacific Decadal Oscillation (PDO). The ENSO and the PDO are climate signals from the oceans and can trigger pronounced changes in climate across the world (Zhang *et al* 2013, Sun *et al* 2016). The variability in precipitation extremes observed in central China can be attributed to the influence of the ENSO: a decrease in precipitation extremes occurs in positive ENSO years (Xiao *et al* 2017). Ouyang *et al* (2014) reported an overall decrease in precipitation during El Niño/PDO warm-phase periods and an increase in precipitation during La Niña/PDO cool-phase periods across most of China. The ENSO has been shown to have an extremely strong and robust influence on seasonal rainfall in East Asia, which has been mainly ascribed to the interactions between the ENSO and the East Asian summer and winter monsoon (Zhou and Wu 2010, Karori *et al* 2013, Ying *et al* 2014). Overall, it is believed that the ENSO and PDO signals may be the source of changes in the spatial and temporal distribution of precipitation. The objectives of this study are therefore to: (1) investigate changes in the spatial heterogeneity and temporal distribution of precipitation over the past five decades in China; and (2) examine the mechanisms (ENSO, PDO, large-scale atmospheric circulation, etc) underlying these changes.

2. Data and methods

2.1. Data

In this study, we obtained the observed daily precipitation data for the period 1957–2014 from the National Meteorological Information Center of the China Meteorological Administration. This dataset is constructed from over 2400 station observations across China at a resolution of $0.5^\circ \times 0.5^\circ$ (Shen *et al* 2010). Monthly PDO and ENSO indices were taken from the Global Climate Observing System Working Group on Surface Pressure (http://esrl.noaa.gov/psd/gcos_wgsp/Timeseries). Rainfall variability may be strongly associated with different stages of the ENSO cycle. We

investigated the influence of the ENSO index from the preceding winter, calculated from the December–January–February Niño 3.4. The wind fields, geopotential-height fields, specific humidity, and surface pressure were obtained from the first National Centers for Environmental Prediction/National Center for Atmospheric Research (NCEP/NCAR) reanalysis (hereafter, NCEP1) (Kalnay *et al* 1996). The NCEP1 global reanalysis provides data at a horizontal resolution of $2.5^\circ \times 2.5^\circ$ at different pressure levels. To investigate atmospheric water-vapor transport, we calculated the vertically integrated water-vapor flux from the surface to 300 hPa pressure and the corresponding water-vapor flux divergence during the summer from the data for wind fields, specific humidity, and surface pressure.

2.2. Analysis methods

Three precipitation indices—the number of wet days, the number of very wet days, and the fraction of precipitation due to very wet days (R95pTOT)—were applied to investigate variations in precipitation. Wet days are defined as days with more than 0.1 mm precipitation. Very wet days are defined as days with more precipitation than the 95th percentile of wet-day precipitation, as measured over the period 1961–1990. R95pTOT indicates the percentage of total precipitation that occurs on very wet days (Karl *et al* 1999).

The nonparametric Mann–Kendall test was used to test the statistical significance of the trends in precipitation indices at each grid point (Mann 1945), and the trend magnitudes were estimated with Sen’s slope estimator (Sen 1968). A 5% significance level was used in all significance tests. China was divided into eight subregions (figure 1), and the changes in the region mean and spatial variance in the eight subregions and mainland China were estimated. The division into subregions followed that of Shi and Xu (2007), and takes into consideration both the administrative divisions and the characteristics of the Chinese monsoon climate.

To assess the role of climate variability (i.e. the effects of the ENSO and the PDO), we linearly detrended the time series within the study period to minimize the effect of any long-term trends or cycles. This is a common method that has been used in previous

studies (Douville 2006, Sutton and Dong 2012, King *et al* 2016). We then calculated the correlation coefficients between the time series for precipitation and the time series for the ENSO and PDO indices. We also used a composite analysis method, similar to that used by Zhang *et al* (2010), to provide a direct view of the possible influence of modes of large-scale variability on the spatial and temporal variations in precipitation. From the period 1957–2014, we first selected the years with the five highest and five lowest values on the ENSO and PDO indices. We computed the 5 year averages for the precipitation indices (P_{high} and P_{low}) for the high- and low-index years. We then calculated the difference in those averages ($P_{\text{high}} - P_{\text{low}}$) to indicate the influence of ENSO and PDO signals and used two-sided Student's *t* tests to determine whether the composite differences were statistically significant. We looked into the possible influence of modes of large-scale variability on the spatial and temporal variations in precipitation extremes; the related wind fields, water vapor transmission, and geopotential height fields are examined to explain the mechanisms underlying the influence of the ENSO and the PDO.

3. Results

3.1. Spatial patterns and trends in precipitation indices

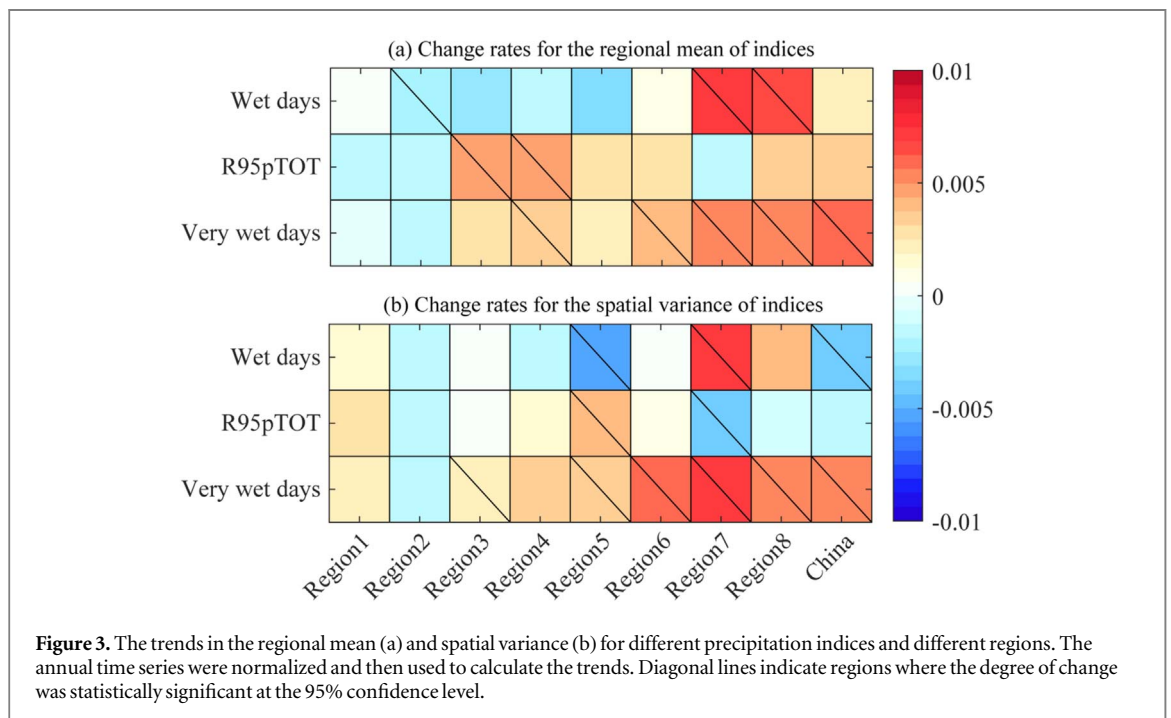
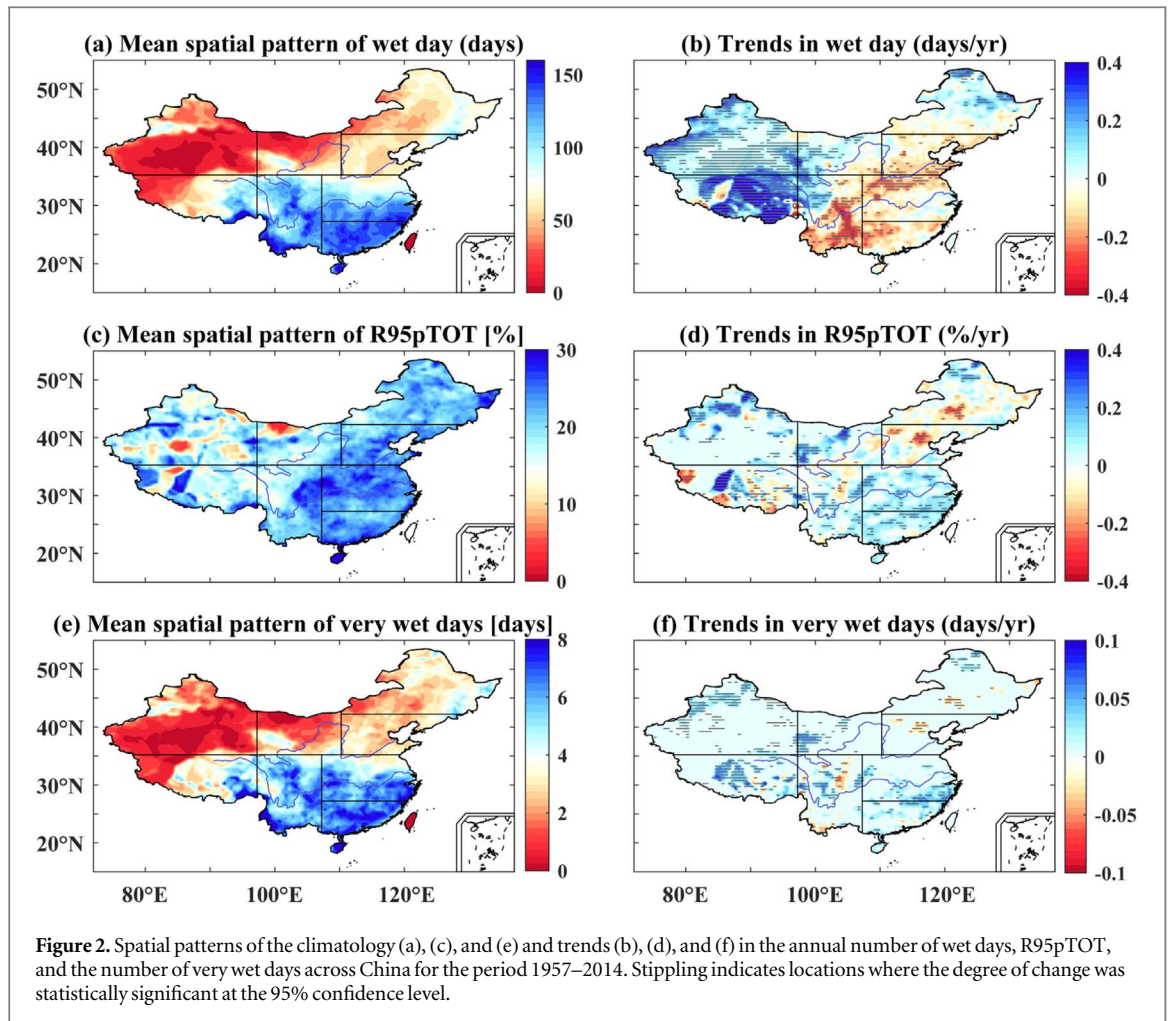
Figure 2 shows the spatial distributions of the mean and the mean annual changes for three precipitation indices (number of wet days, R95pTOT, and the number of very wet days) across China. The number of wet days and very wet days decreased gradually from southeastern to northwestern China. The trends in the number of wet days were spatially non-uniform (figure 2(b)); statistically significant downward trends were found in the large regions of eastern China. In contrast, large areas of western China and some of the northeastern regions showed statistically significant upward trends. The annual changes ranged from -0.4 to 0.4 d yr^{-1} , with the strongest downward trends located in Southwest China (region 4) and the strongest upward trends located in the southern region of the Tibetan Plateau (region 7). The number of very wet days increased in Northwest China (region 6 and region 8), Tibetan Plateau (region 7), Jianghuai (region 3) and South China (region 4) (figure 2(f)), with extreme precipitation events contributing a greater fraction of the total precipitation (figure 2(d)). In Jianghuai, South China and some regions over Northwest China (region 6 and region 8), statistically significant upward trends were found for both R95pTOT and very wet days. However, the opposite trends were observed for R95pTOT in Northeast China (region 1).

3.2. Regional mean and spatial changes in the precipitation indices

In addition to the non-uniform spatial changes in precipitation over China, the regional mean and spatial variance of precipitation show changes over time. Extremes in climate can easily trigger tremendous damage to both social and natural systems, hence our focus is on the regional mean and spatial variance of the number of wet days and very wet days, and R95pTOT. The final column of figures 3(a) and (b) show that the regional means of R95pTOT and the number of wet days across China increased over the period 1957–2014, whereas the spatial variance decreased over the same period. However, the regional mean and spatial variance of the number of very wet days showed a statistically significant upward tendency. At the regional scale, Jianghuai (region 3), South China (region 4), and Southwest China (region 5) experienced an increase in the number of extreme events over this period, with upward trends in the number of very wet days but downward trends in the number of wet days; this pattern contributed to the increase in R95pTOT. In the Tibetan Plateau (region 7) and the west of Northwest China (region 8), there was a clear upward trend in both the number of wet days and the number of very wet days. The spatial variance of very wet days increased in most regions except North China (region 8) (figure 3(b)), indicating that the increase in extreme events mainly occurred in the grids with a higher risk of extreme precipitation.

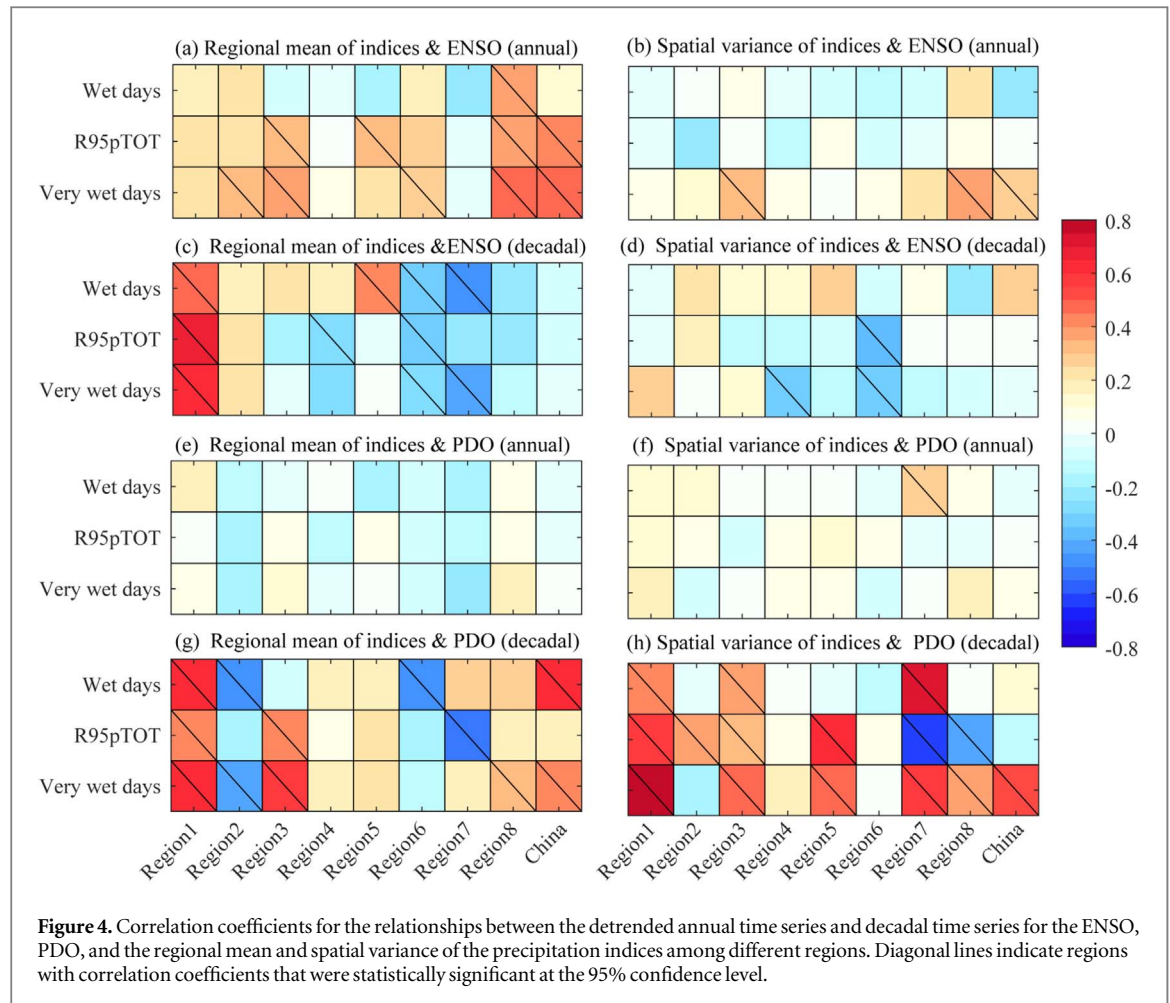
3.3. The influence of the ENSO and the PDO

Figure 4 shows the correlation coefficients between the precipitation indices and the ENSO/PDO at annual and decadal scales. At the annual time scale, the regional mean of R95pTOT and the number of very wet days across China were positively correlated with the ENSO, and the spatial variance of the number of very wet days was also positively correlated with the ENSO. The influence of the ENSO on R95pTOT was mainly concentrated in Jianghuai (region 3), Southwest China (region 5), and the west of Northwest China (region 8). Overall, the ENSO mainly modulated the inter-annual variation of extreme events, and statistically significant correlation coefficients with the number of very wet days were found in most regions (figure 4(a)). However, the inter-decadal variations were controlled by the PDO, which showed clear correlations at decadal time scales. There was a positive correlation between the PDO and the regional mean and spatial variance of the number of very wet days across China, but a negative correlation with the spatial variance of R95pTOT (figures 4(g) and (h)). Moreover, the effects of the PDO were zonal; the precipitation mean and extremes exhibited spatially opposite patterns during different PDO phases because of the modulation of different atmospheric circulation systems. During the positive PDO phase, a



weakened and southward western Pacific subtropical high and significant northerly anomaly caused a weakening of the East Asia summer monsoon, and a

consequent pattern of ‘southern flood/northern drought’ (Fu *et al* 2009, Ouyang *et al* 2014). The significant negative correlation with PDO in North



China (region 2) and significant positive correlation with PDO in the Jianghuai region (region 3) was consistent with this pattern (figure 4(g)). During the negative PDO phase, the thermal contrast between Northeast China (region 1) and the oceans is reduced because of warming sea surface temperature in the North Pacific (Han *et al* 2015). Consequent weakening of the northeast Asian summer monsoon may cause a reduction in the water-vapor flux and thus affect precipitation over Northeast China (region 1, figure 4(g)).

We applied a composite analysis method to assess the influence of the ENSO and the PDO on changes in precipitation characteristics. Figure 5 shows the composite differences between the average of the five strongest El Niño and La Niña years, based on Niño 3.4 values. Compared with La Niña years, the frequency of wet days and very wet days in El Niño years tended to be greater over large areas of southeastern and northeastern China. The results indicate that there was a greater probability of extreme precipitation events occurring in El Niño years than La Niña years in these regions. Over the southern part of North China and the northern part of Jianghuai, the frequency of wet days in El Niño years was relatively lower. R95pTOT was greater in El Niño years than La Niña years in some grids scattered in Jianghuai and the

west of Northwest China, with difference values ($P_{\text{high}} - P_{\text{low}}$) of up to 5%.

The frequency of wet days during positive PDO years increased in large parts of southeastern China and some grid locations in northeastern China and the west of Northwest China (figure 5(b)), although most of these changes were not statistically significant. The number of wet days showed decreases during the positive PDO phase across North China. For most grid locations in Southwest China, the middle and upper Yangtze River basin, and Northeast China, the values for the number of very wet days tended to be lower during the negative PDO phase than during the positive PDO phase (figure 5(f)).

3.4. Effects of large-scale atmospheric circulation

Figures 6(a) and (b) show the integrated atmospheric water-vapor flux and the mean atmospheric water-vapor flux divergence during the summer for the strongest five El Niño and La Niña years. The increase in wet days and very wet days over southeastern China during the El Niño phase might be a response to the increase in atmospheric water-vapor flux and decrease in water-vapor divergence there during the summer. Similarly, a decrease in water-vapor flux and an increase in water-vapor divergence may contribute to the decrease in the frequency of wet days in northern

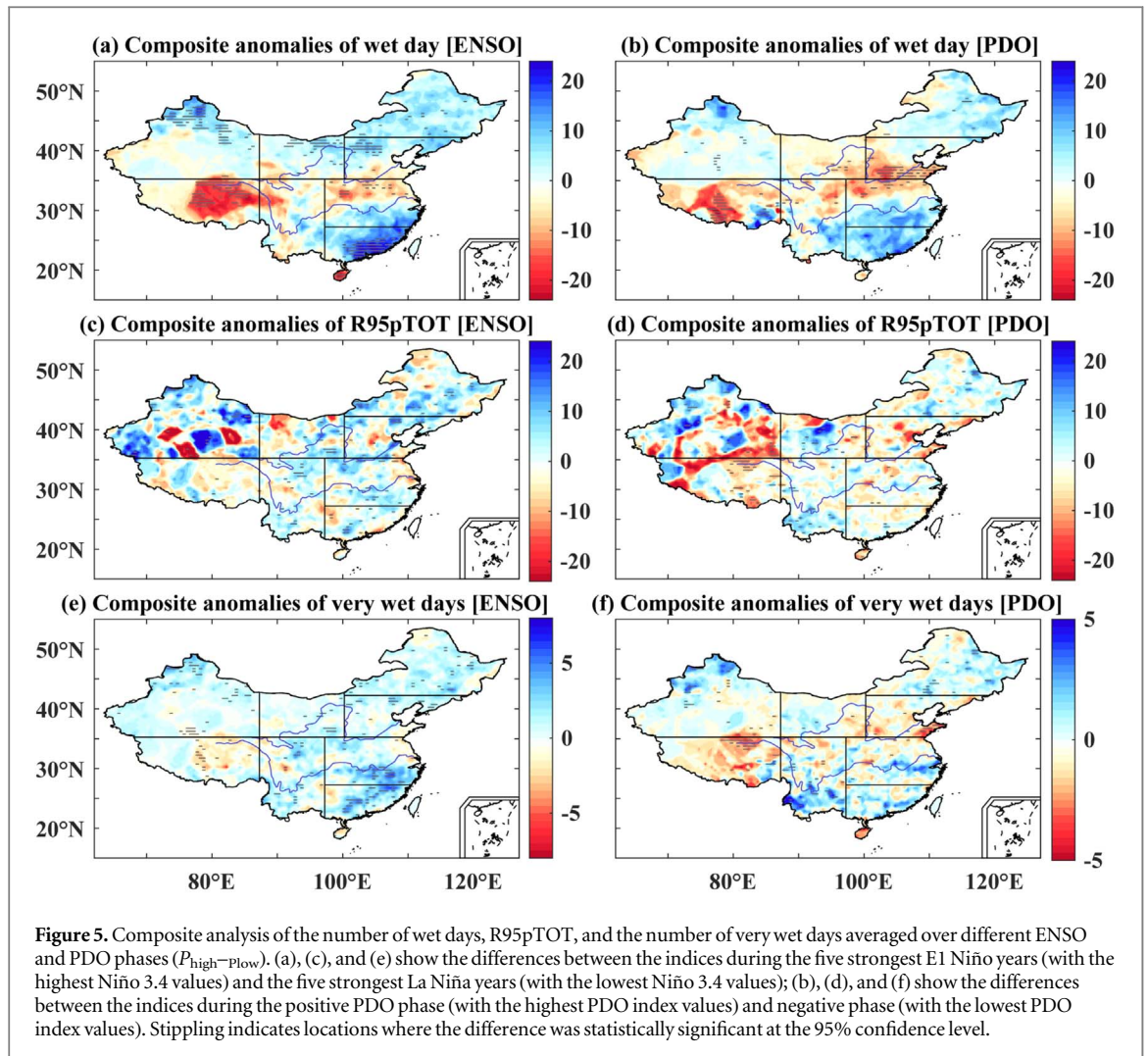


Figure 5. Composite analysis of the number of wet days, R95pTOT, and the number of very wet days averaged over different ENSO and PDO phases ($P_{\text{high}} - P_{\text{low}}$). (a), (c), and (e) show the differences between the indices during the five strongest El Niño years (with the highest Niño 3.4 values) and the five strongest La Niña years (with the lowest Niño 3.4 values); (b), (d), and (f) show the differences between the indices during the positive PDO phase (with the highest PDO index values) and negative phase (with the lowest PDO index values). Stippling indicates locations where the difference was statistically significant at the 95% confidence level.

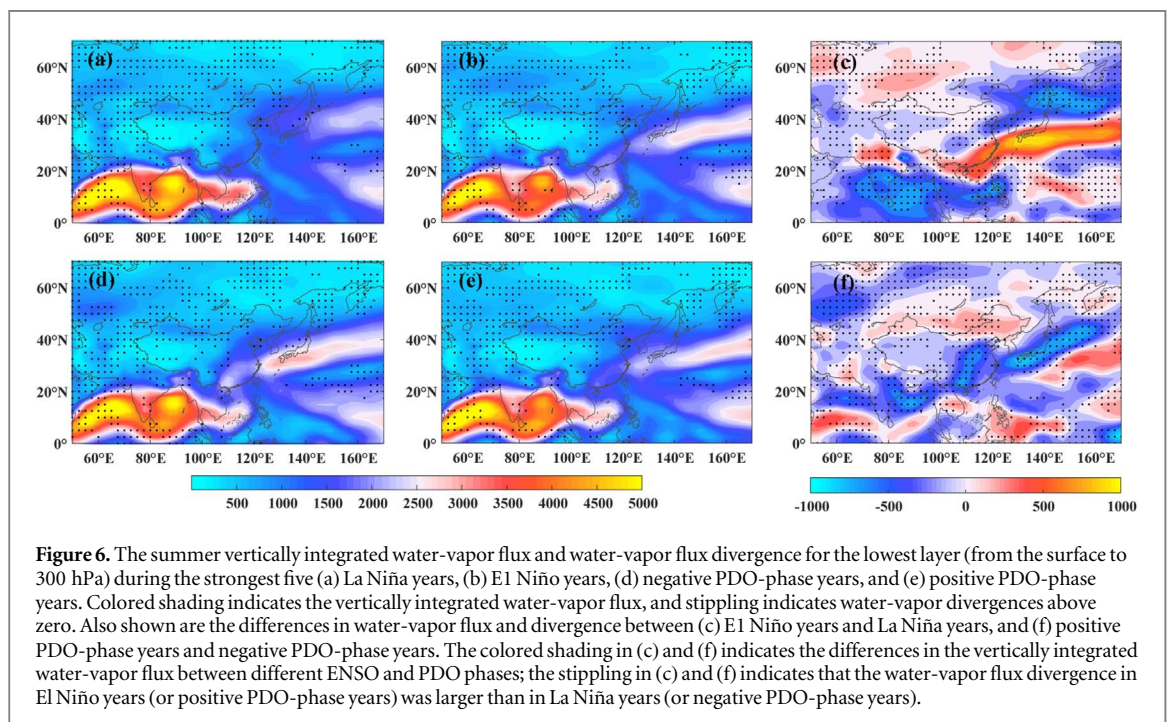
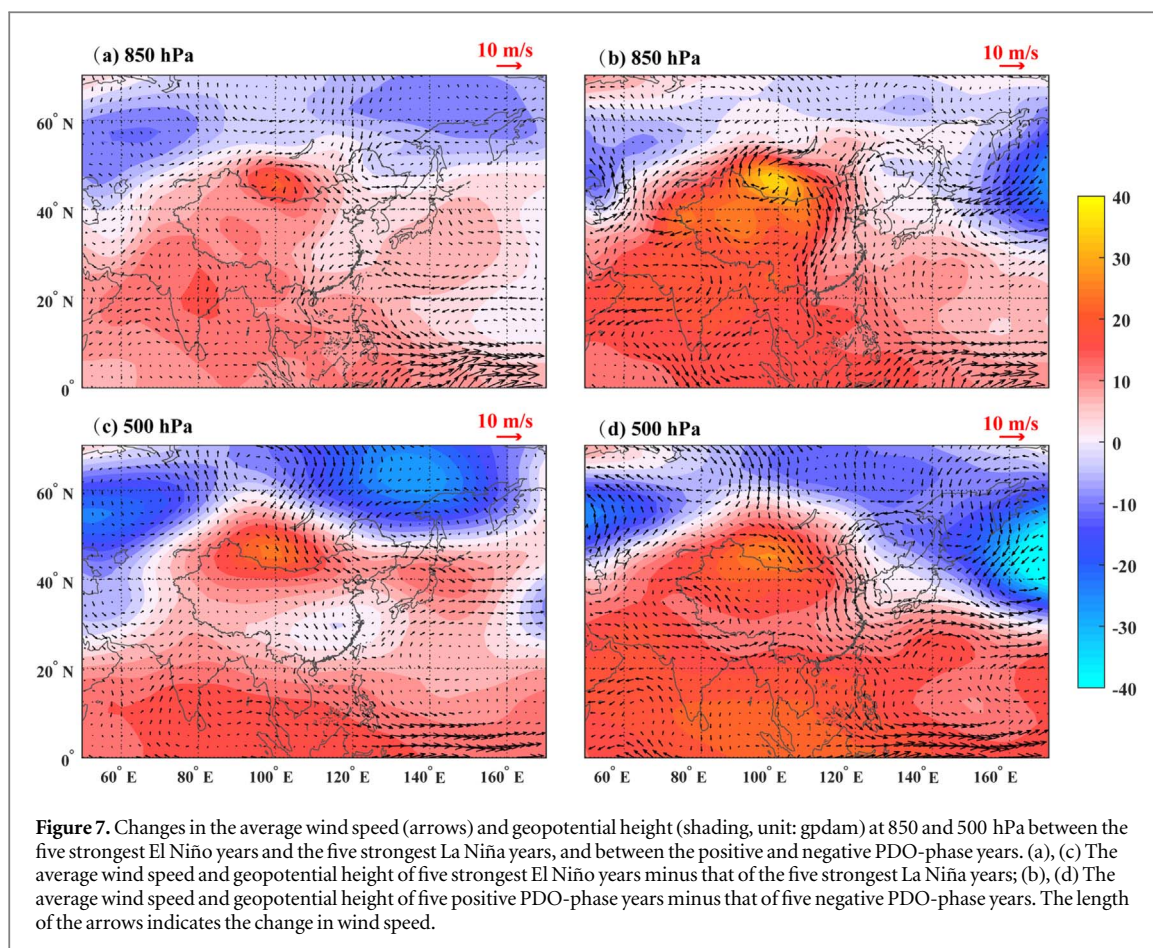


Figure 6. The summer vertically integrated water-vapor flux and water-vapor flux divergence for the lowest layer (from the surface to 300 hPa) during the strongest five (a) La Niña years, (b) El Niño years, (d) negative PDO-phase years, and (e) positive PDO-phase years. Colored shading indicates the vertically integrated water-vapor flux, and stippling indicates water-vapor divergences above zero. Also shown are the differences in water-vapor flux and divergence between (c) El Niño years and La Niña years, and (f) positive PDO-phase years and negative PDO-phase years. The colored shading in (c) and (f) indicates the differences in the vertically integrated water-vapor flux between different ENSO and PDO phases; the stippling in (c) and (f) indicates that the water-vapor flux divergence in El Niño years (or positive PDO-phase years) was larger than in La Niña years (or negative PDO-phase years).



China. Over southeastern China, the water-vapor flux was lower during the positive PDO phase than during the negative PDO phase (figure 6(f)) but the number of very wet days increased, which may be related to the decrease in water-vapor divergence. A decrease in water-vapor divergence is conducive to the convergence of water vapor.

Figure 7 shows a northerly wind anomaly in El Niño years over southeastern China. The concurrence of weaker winds and high water-vapor flux could result in the persistence and accumulation of water content and hence an increase in the number of wet days and extreme events in this region. An examination of the 500 hPa geopotential height distribution suggests that the subtropical high tended to be weaker and more southward in El Niño years (figure 7(c)). The weakening of winds in the south and the southward movement of the subtropical high could simultaneously restrict the northward water vapor and result in the reduction in the number of wet days in northern China. During the positive PDO phase, a cyclonic circulation anomaly occurred in northwestern China (figure 7(b)), and a northerly wind anomaly appeared in eastern China, which resulted in the convergence of cold air from the north with warm air from the south. Consequently, one might expect an increase in the number of wet days in southern China during the positive PDO phase, as shown in figure 4(b). In northeastern China, an easterly wind

anomaly was observed during the positive PDO phase, which could result in warmer and wetter air being transported there from the sea.

4. Discussion and conclusions

We have presented here an analysis of the changing spatial and temporal variability in precipitation over mainland China during the period 1957–2014. The influence of the ENSO, the PDO, and related atmospheric circulation variables were examined to explore the underlying mechanisms driving these changes. Our results show that the change in the number of wet days and very wet days was not spatially uniform across China, but instead showed strong regional variations. The number of wet days showed statistically significant downward trends in the North China, Jianghuai, South China, and Southwest China regions but increased on the Tibetan Plateau and in Northwest China. It should be noted that, despite the overall decrease in precipitation in the Jianghuai region and South China, the risk of heavy precipitation events might not be reduced but may even be increased. Large regions of southeastern China generally featured an increased contribution of extreme events to overall precipitation amounts, as demonstrated by statistically significant upward trends in R95pTOT and the number of very wet days. These spatially non-uniform

trends contributed to changes in the spatial variability of precipitation. In the context of global warming, more extreme precipitation occurred concurrently with an increase in the number of very wet days, which was consistent with previous studies (Min *et al* 2011, Fischer and Knutti 2015, Miao *et al* 2016b). These results suggest that extreme precipitation has become more homogenous and widespread across mainland China.

The ENSO and the PDO are major factors that control the variability of precipitation at a global scale because they modulate variability in global atmospheric circulation. Our results suggest that the spatial variability and temporal distribution of precipitation over China are correlated with the ENSO and the PDO. The influence of the ENSO and the PDO had zonal characteristics. During E1 Niño years, wet days and extreme precipitation events tended to occur more frequently in southeastern China, but there were fewer wet days in northern China. The concurrence of higher water-vapor flux, weaker winds, and changes in the subtropical high in E1 Niño years could enhance the differences in precipitation variability between southern and northern China and hence result in greater spatial variability. The strong decrease in southerly winds in the positive PDO phase likely contributed to the reduction in the number of wet days in northern China and the increase in wet days in southeastern China. The reduction in water-vapor divergence was conducive for the formation of extreme weather events in southeastern China during the positive PDO phase. Furthermore, the easterly wind anomaly and positive water-vapor content in northeastern China could simultaneously increase the number of wet days and the amount of extreme precipitation in that region. These non-uniform changes also inevitably contributed to the overall changes in spatial variability.

In summary, the ENSO, the PDO, and large-scale atmospheric circulation are likely to be important factors in the variability of precipitation on both spatial and temporal scales. In this study, we simply divided the ENSO and PDO phases on the basis of the annual values of the ENSO and PDO indices. Nevertheless, the different types of ENSO events and different timing of the ENSO events resulted in the observed asymmetries and nonlinearities in the influence of the ENSO on precipitation variability (Karori *et al* 2013, Zhang *et al* 2013). ENSO and PDO signals can interact with each other when the ENSO and the PDO are in phase, which intensifies their influence on climate anomalies (Gershunov and Barnett 1998). In addition, other factors, such as urbanization, land use, and topographic heterogeneity, can significantly affect local microclimates and the formation of precipitation, and thereby also affect the spatial heterogeneity and temporal distribution of precipitation (Ghosh *et al* 2011, Liu *et al* 2014, Liu *et al* 2015). Further analysis is required to investigate the underlying mechanisms

and the interactions between the different factors. The observed spatial heterogeneity and temporal inequality in precipitation indicates that there is a high risk of different natural hazards occurring in different regions throughout the year. Systematic examination of changes in the spatial variation and temporal distribution of precipitation in future climate scenarios is essential for the management and mitigation of natural hazards in China.

Acknowledgments

This research was supported by the National Natural Science Foundation of China (No. 41622101, No. 41877155), the National Key Research and Development Program of China (No. 2016YFC0501604) and the Fundamental Research Funds for the Central Universities. We are also grateful to National Meteorological Information Center of the China Meteorological Administration (NMIC, <http://data.cma.cn>), Global Climate Observing System Working Group on Surface Pressure (WG-SP, http://www.esrl.noaa.gov/psd/gcos_wgsp/Timeseries) for providing the observed climate data and climate signals from the oceans, as well as the National Centers for Environmental Prediction/National Center for Atmospheric Research (NCEP/NCAR) for providing the reanalysis dataset.

ORCID iDs

Chiyuan Miao  <https://orcid.org/0000-0001-6413-7020>

References

- Donat M G *et al* 2013 Updated analyses of temperature and precipitation extreme indices since the beginning of the twentieth century: the HadEX2 dataset *J. Geophys. Res.-Atmos.* **118** 2098–118
- Douville H 2006 Detection-attribution of global warming at the regional scale: how to deal with precipitation variability? *Geophys. Res. Lett.* **33** L02701
- Fischer E M and Knutti R 2015 Anthropogenic contribution to global occurrence of heavy-precipitation and high-temperature extremes *Nat. Clim. Change* **5** 560–4
- Fu G B, Charles S P, Yu J J and Liu C M 2009 Decadal climatic variability, trends, and future scenarios for the north China plain *J. Climate* **22** 2111–23
- Gershunov A and Barnett T P 1998 Interdecadal modulation of ENSO teleconnections *Bull. Amer. Meteor. Soc.* **79** 2715–25
- Ghosh S, Das D, Kao S C and Ganguly A R 2011 Lack of uniform trends but increasing spatial variability in observed Indian rainfall extremes *Nat. Clim. Change* **2** 86–91
- Han T, Chen H and Wang H 2015 Recent changes in summer precipitation in Northeast China and the background circulation *Int. J. Climatol.* **35** 4210–9
- Kalnay E *et al* 1996 The NCEP/NCAR 40-year reanalysis project *Bull. Am. Meteor. Soc.* **77** 437–71
- Karl T R, Nicholls N and Ghazi A 1999 Clivar/GCOS/WMO workshop on indices and indicators for climate extremes workshop summary *Clim. Change* **42** 3–7

- Karori M A, Li J P and Jin F F 2013 The asymmetric influence of the two types of El Nino and La Nina on summer rainfall over Southeast China *J. Clim.* **26** 4567–82
- King A D, Karoly D J and van Oldenborgh G J 2016 Climate change and El Nino increase likelihood of Indonesian heat and drought *Bull. Am. Meteor. Soc.* **97** S113–7
- Liu M *et al* 2014 Is southwestern China experiencing more frequent precipitation extremes? *Environ. Res. Lett.* **9** 064002
- Liu M X, Xu X L and Sun A 2015 Decreasing spatial variability in precipitation extremes in southwestern China and the local/large-scale influencing factors *J. Geophys. Res.-Atmos.* **120** 6480–8
- Ma S, Zhou T, Dai A and Han Z 2015 Observed changes in the distributions of daily precipitation frequency and amount over China from 1960–2013 *J. Clim.* **28** 6960–78
- Mann H B 1945 Nonparametric tests against trend *Econometrica* **13** 245–59
- Miao C, Kong D, Wu J and Duan Q 2016b Functional degradation of the water–sediment regulation scheme in the lower yellow river: spatial and temporal analyses *Sci. Total Environ.* **551–552** 16–22
- Miao C, Sun Q, Borthwick A G L and Duan Q 2016a Linkage between hourly precipitation events and atmospheric temperature changes over China during the warm season *Sci. Rep.* **6** 22543
- Min S K, Zhang X, Zwiers F W and Hegerl G C 2011 Human contribution to more-intense precipitation extremes *Nature* **470** 378–81
- Ouyang R *et al* 2014 Linkages between ENSO/PDO signals and precipitation, streamflow in China during the last 100 years *Hydrol. Earth Syst. Sci.* **18** 3651–61
- Rajah K *et al* 2014 Changes to the temporal distribution of daily precipitation *Geophys. Res. Lett.* **41** 8887–94
- Sen P K 1968 Estimates of the regression coefficient based on Kendall's Tau *J. Am. Stat. Assoc.* **63** 1379–89
- Shen Y, Xiong A, Wang Y and Xie P 2010 Performance of high-resolution satellite precipitation products over China *J. Geophys. Res.* **115** D02114
- Shi X and Xu X 2007 Regional characteristics of the interdecadal turning of winter/summer climate modes in Chinese mainland *Chin. Sci. Bull.* **52** 101–12
- Sun Q, Miao C, AghaKouchak A and Duan Q 2016 Century-scale causal relationships between global dry/wet conditions and the state of the pacific and atlantic oceans *Geophys. Res. Lett.* **43** 6528–37
- Sun Q *et al* 2018 A review of global precipitation datasets: data sources, estimation, and intercomparisons *Rev. Geophys.* **56** 79–107
- Sutton R T and Dong B 2012 Atlantic ocean influence on a shift in European climate in the 1990s *Nat. Geosci.* **5** 788–92
- Xiao M, Zhang Q and Singh V P 2017 Spatiotemporal variations of extreme precipitation regimes during 1961–2010 and possible teleconnections with climate indices across China *Int. J. Climatol.* **37** 468–79
- Xu Z, Fan K and Wang H 2015 Decadal variation of summer precipitation over China and associated atmospheric circulation after the late 1990s *J. Climate* **28** 4086–106
- Ying K *et al* 2014 Interannual variability of autumn to spring seasonal precipitation in eastern China *Clim. Dyn.* **45** 253–71
- Zhang Q, Li J, Singh V P, Xu C Y and Deng J 2013 Influence of ENSO on precipitation in the East River basin, south China *J. Geophys. Res.- Atmos.* **118** 2207–19
- Zhang X, Wang J, Zwiers F W and Groisman P Y 2010 The influence of large-scale climate variability on winter maximum daily precipitation over North America *J. Clim.* **23** 2902–15
- Zhou L T and Wu R 2010 Respective impacts of the East Asian winter monsoon and ENSO on winter rainfall in China *J. Geophys. Res.- Atmos.* **115** 753–65